Growing Sapphire Single Crystals by the Vernouil Method Using Town Gas and Their Some Crystallographic Features

Growing Sapphire Single Crystals by the Vernouil Method Using Town Gas and Their Some Crystallographic Features*

Mikio YAMAMOTO, Seizô ARINO** and Tokujirô SATÔ

The Research Institute for Iron, Steel and Other Metals

(Received January 26, 1971)

Synopsis

Glowing sapphire crystals by the Vernouil method using town gas instead of hydrogen gas were tried. It is known that small but good crystals are obtained in spite of a relatively rough control of gas pressures. [0001], [10$\bar{1}$0], and [1$\bar{2}$10] standard stereographic projections are constructed on the basis of calculated angles between various crystal plane of sapphire crystal. [0001] and [11$\bar{2}$0] etch pits and corresponding light figures of sapphire crystals are observed and it is shown that the orientation determination of them by the light-figure method can be made simply and accurately.

I. Introduction

Although sapphire or α-Al_2O_3 crystal is one of very widely known oxide crystals, its crystallographic features, imperfections, and properties have not yet been studied in detail. Properties of dislocations in it is not completely clarified, although several studies have so far been made.(1)

Now, we have studied on the growth feature of sapphire crystals by the Vernouil method using town gas instead of hydrogen gas and on their some crystallographic features, of which the results are reported in this paper.

II. Growing sapphire crystals

We have grown sapphire crystals by the Vernouil method. Because of their low melting point, town gas has been employed instead of hydrogen gas. The optimum condition of grown sapphire crystals using town gas has been found to be as follows: The time rate of supplying the raw material powder is 0.25 g/min, the time rate of supplying town gas is 13 l/min, the time rate of supplying oxygen gas is 10 l/min, and the growing rate of the crystal is 13 mm/min.

Since we employed town gas instead of hydrogen gas as just said, bowls obtained show necking and roughness on their side surfaces (Fig. 1), including also bubbles (Fig. 2). Further, they have thermal strain, which produces many

* The **1475th** report of the Research Institute for Iron, Steel and Other Metals.

** Now at the Nippon-Victor Co. Ltd., Yokohama.

(1) See e.g. Y. Takano, Jap. J. Appl. Phys., **9** (1970), 847.

Fig. 1.

Fig. 2.

Fig. 1. Appearance of a sapphire bowl grown using town gas-oxygen flame.
Fig. 2. Bubble included in a sapphire crystal grown using town-gas-oxygen flame.

cracks, so that they are not halfed in a simple way. All of these defects are resulted from the difficulty of controlling exactly the flow rate of town gas. It is to be noted, however, that etch pits revealed on their surfaces, which will be described later, have the density of $10^5/cm^2$, which is not so much deviated from the values found with bowls produced using a usual oxygen-hydrogen flame.

From many Vernouil experiments performed by us, it can be inferred as follows: During crystal growing, since the spitz of the seed crystal is within the highest temperature portion of the flame, a very thin molten layer exists there. The raw material powder falled down is heated to a high temperature by a town gas-oxygen gas flame and melts locally at the spitz of the seed crystal. On the other hand, the under portion of the seed crystal is at temperatures under the melting point, so that the heat flows from the spitz to the base of the seed crystal, which then produces the undercooling of the molten layer. In order to maintain always a constant degree of super-cooling, the flow rate must be kept very rigorously. Also, it is necessary to homogenize the heat distribution within the crystal, which is achieved by rotating the seed crystal.

It can be known from the above-described experiments that, in the case of using town gas instead of hydrogen gas, small but good sapphire crystals are obtained in spite of a relatively rough control of gas pressure.

III. Standard stereographic projection of sapphire crystal

The space lattice of sapphire crystal is rhombohedral-hexagonal, the space group being D_{3d}^6=R3C[(2)]. As its unit cell, we can take both of structural and

(2) M.I. Kronberg: Acta Met., **5** (1957), 507.

Table 1. Calculated angles between various crystal planes of sapphire.

	0001	$10\bar{1}0$	$11\bar{2}0$	$10\bar{1}4$	$20\bar{2}5$	$10\bar{1}1$	$40\bar{4}1$	$01\bar{1}2$	$02\bar{2}1$	$11\bar{2}6$	$22\bar{4}9$	$11\bar{2}3$	$22\bar{4}3$	$44\bar{8}3$	$21\bar{3}1$	$62\bar{8}1$	$24\bar{6}7$	$12\bar{3}2$
$10\bar{1}0$	90.0																	
$11\bar{2}0$	90.0	30.0																
$10\bar{1}4$	21.5	68.5																
$20\bar{2}5$	32.2	57.8		10.7														
$10\bar{1}1$	57.6	32.4	43.0	36.1	25.4													
$40\bar{4}1$	81.0	9.0	31.2	59.5	48.8	23.4												
$01\bar{1}2$	38.2		57.6	32.4	34.0	47.0												
$02\bar{2}1$	72.4		34.4		59.3	55.6	58.8	34.2										
$11\bar{2}6$	24.5		65.5	12.0				20.5										
$22\bar{4}9$	31.2		58.8		15.7			18.3		6.8								
$11\bar{2}3$	42.3		47.7		20.5	27.3		19.7	38.8	17.9	11.1							
$22\bar{4}3$	61.2		28.8			26.0		32.0	29.7	36.8	30.0	18.9						
$44\bar{8}3$	74.6		15.4				30.0		28.8	50.2	43.4	32.3	13.4					
$21\bar{3}1$			17.3			25.7	19.3	50.4	39.5				18.3	10.7				
$62\bar{8}1$			16.9				14.4	60.3					28.2		9.0			
$24\bar{6}7$					31.6			17.7	27.8			11.0	14.4		32.7	42.6		
$12\bar{3}2$			27.7			36.2		29.9	19.5				10.2					
$13\bar{4}4$			38.2		37.9			19.4	21.5			17.4					6.4	10.5

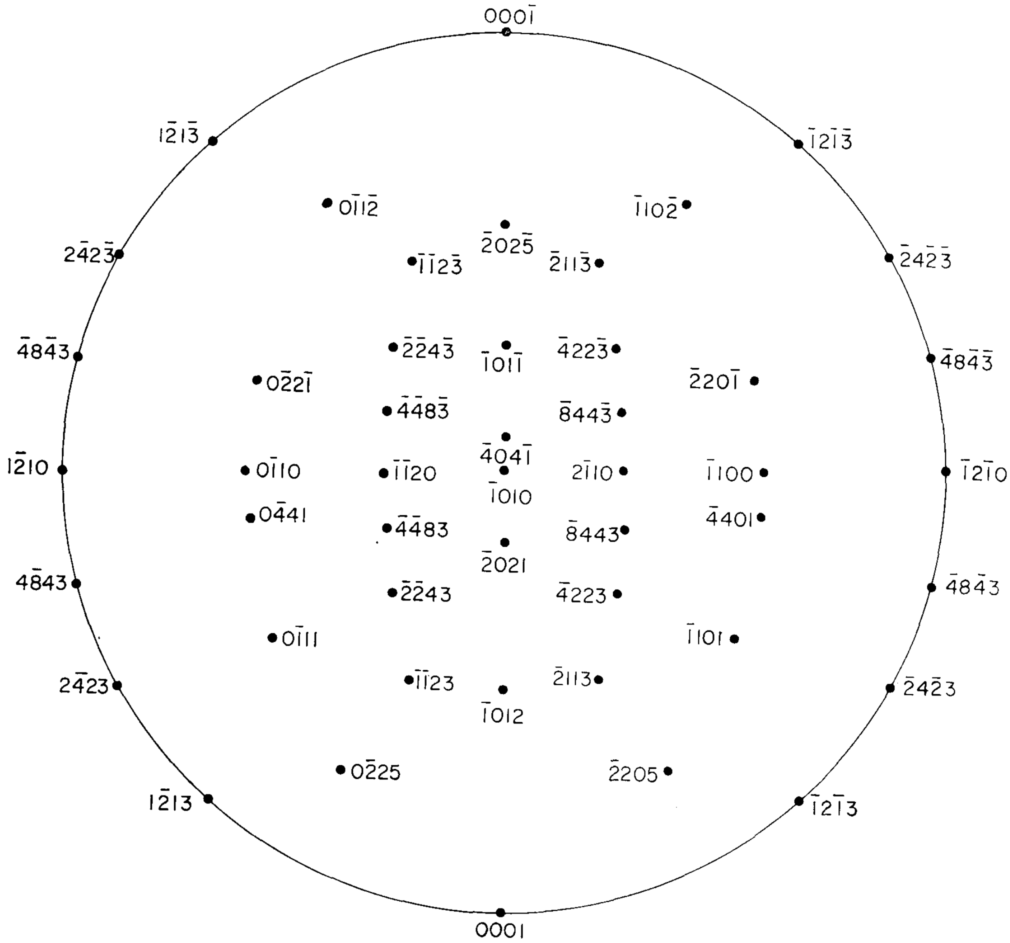

Fig. 3. [0001] stereographic projection of sapphire crystal.

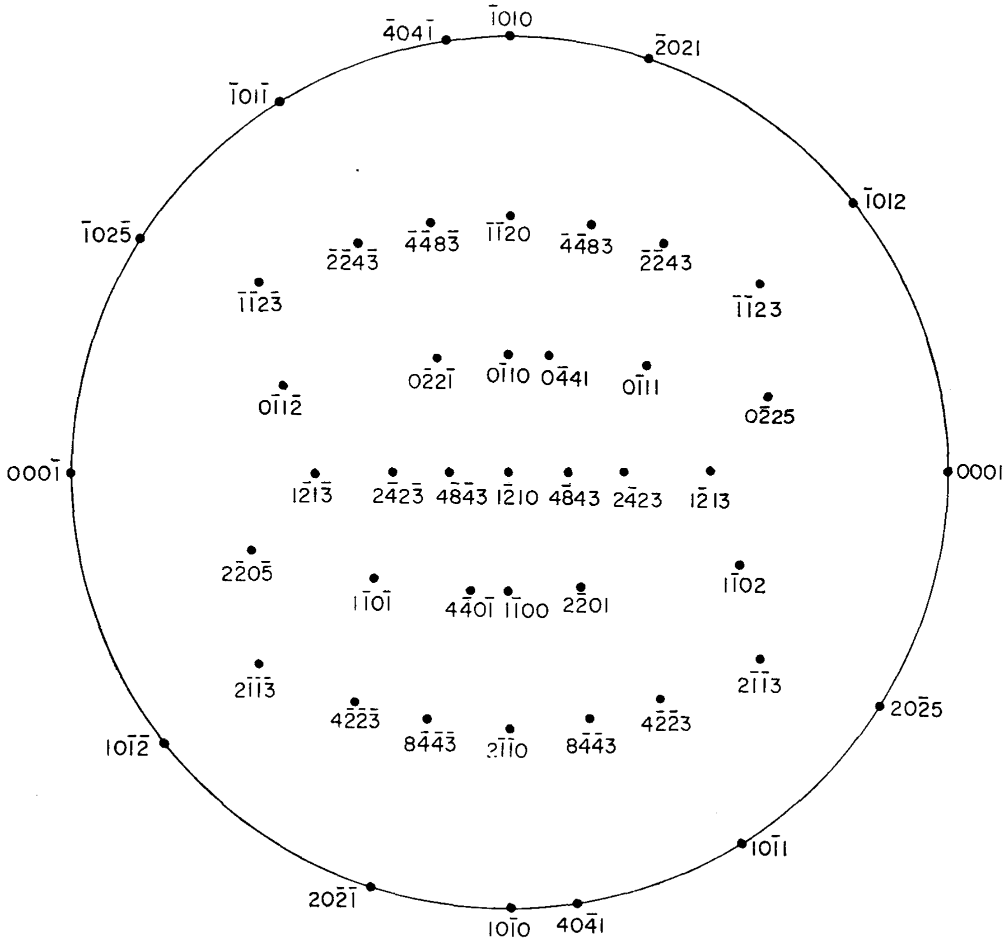

Fig. 4. [$10\bar{1}0$] stereographic projection of sapphire crystal.

morphological ones, each of which is used according to circumstances. The intra-relation of both unit cells are as follows[(3)]:

for the rhombohedral unit cell

structural: a_0=5.12 Å, α=55°17′, n=2;

morphological: a_0=3.49 Å, α=85°45′, n=2,

and for the hexagonal one

structural: A_0=4.75 Å, C_0=12.97 Å, C_0/A_0=2.730, n=6;

morphological: A=4.75 Å, C_0=12.97 Å, C_0/A_0=1.365, n=6.

The just-described relations are employed for the calculation of angles between various crystal planes, using the following formulae:

$$\cos\phi = \frac{h_1h_2+k_1k_2+(1/2)(h_1k_2+h_2k_1)+(3/4)(a^2/c^2)l_1l_2}{\sqrt{\{h_1^2+k_1^2+h_1k_1+(3/4)(a^2/c^2)l_1^2\}\{h_2^2+k_2^2+h_2k_2+(3/4)(a^2/c^2)l_2^2\}}}$$

for the hexagonal unit cell, and

(3) R. Schenplein and P. Gibbs: J. Amer. Ceram. Soc., **43** (1960), 485.

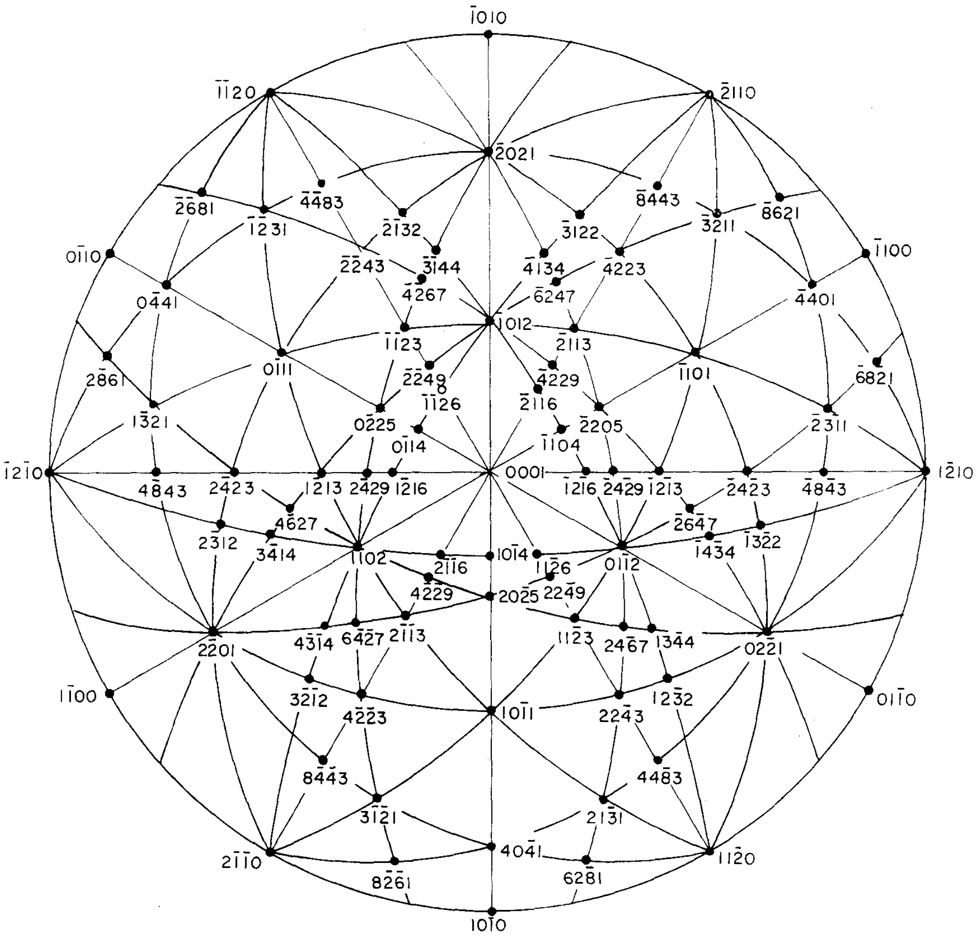

Fig. 5. [11$\bar{2}$0] stereographic projection of sapphire crystal.

$$\cos\phi=\frac{a^2d_1d_2}{V^2}\,[\sin^2\alpha(h_1h_2+k_1k_2+l_1l_2)+(\cos^2\alpha-\cos\alpha)(k_1l_2+k_2l_1$$
$$+l_1h_2+l_2h_1+h_1k_2+h_2k_2]$$

for the rhombohedral one. On the basis of the data shown in Table 1, [0001], [1010], and [11$\bar{2}$0] standard stereographic projections are constructed, which are shown in Figs. 3, 4, and 5, respectively.

IV. Etch pits and corresponding light figures

[0001] and [11$\bar{2}$0] surfaces were cut out from a bowl with the Yamamoto's orientated cutter(4) and it was heated at about 600° C. Subsequently, it was immersed for 25 minutes into the melt of $KHSO_4$ contained in a quartz crucible at about 600° C. After the crystal was cooled down to room temperature, its surfaces were observed under an optical microscope.

Etch pits such as shown in Figs. 6∼8 have been observed on [0001] and [11$\bar{2}$0]

(4) M. Yamamoto, J. Watanabé, and E. Sasaki, Sci Rep. RITU., **A18**, Supplement (1966), 494.

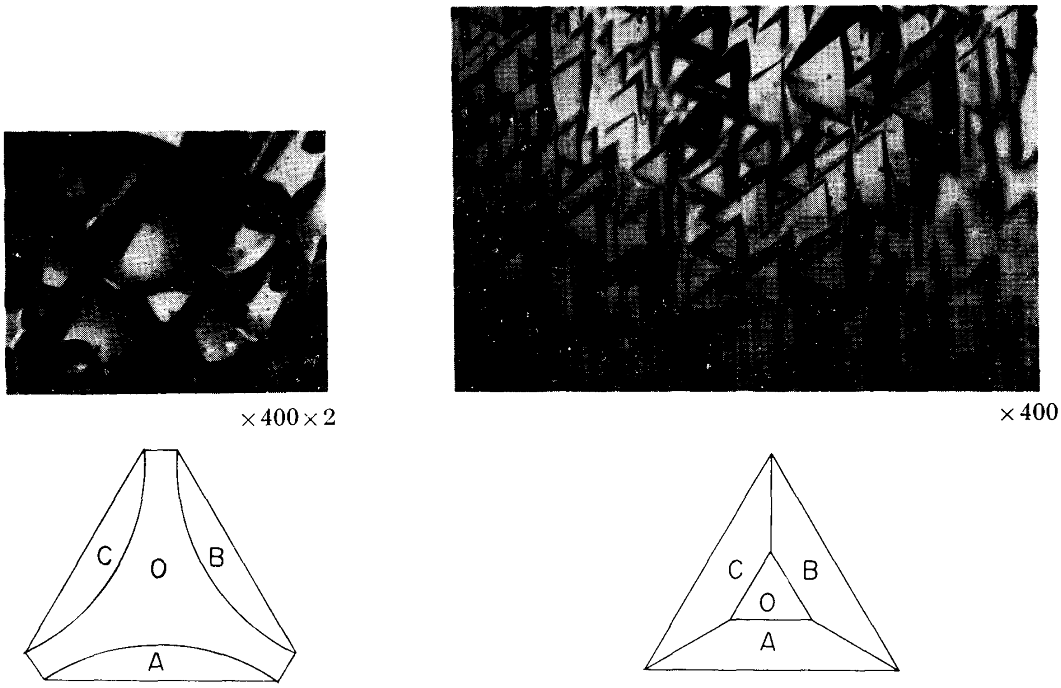

Fig. 6. (0001) etch pits of sapphire crystals.

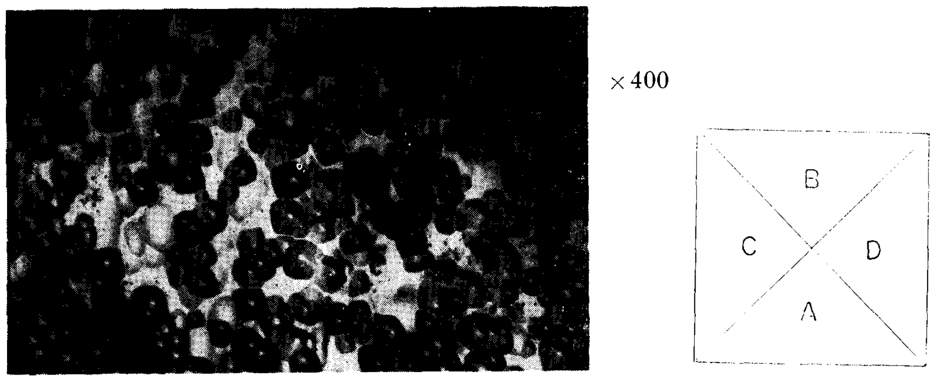

Fig. 7. (11$\bar{2}$0) etch pits of a sapphire and their illustration.

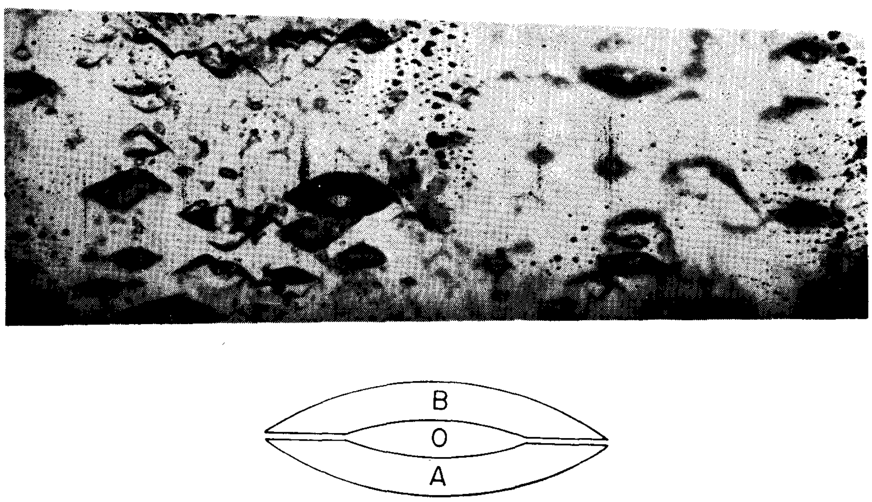

Fig. 8. (10$\bar{1}$0) etch pits of a sapphire crystal and their illustration.

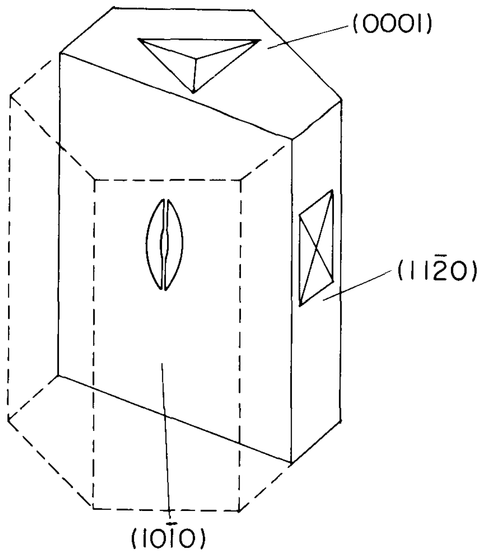

Fig. 9. Spatial relationship among [0001], [11$\bar{2}$0] and [10$\bar{1}$0] etch pits of a sapphire crystal.

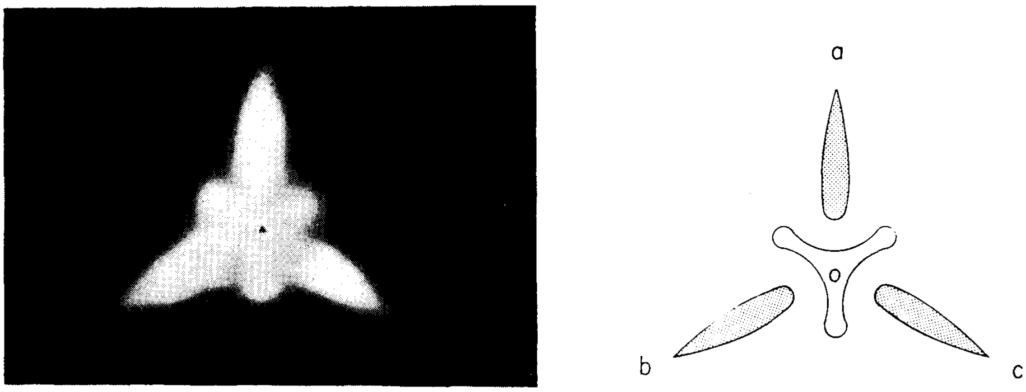

Fig. 10. [0001] light figure of a sapphire crystal and its illustration.

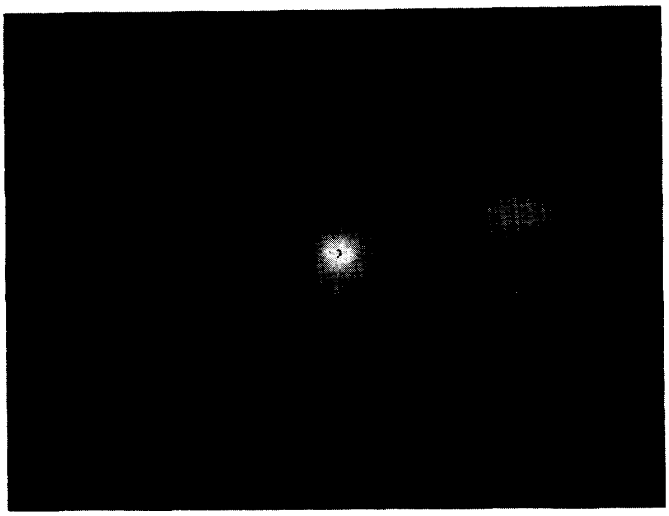

Fig. 11. [11$\bar{2}$0] light figure of sapphire crystal.

Table 2. Angles between various crystal planes of sapphire as measured using (0001) light figure.

Measured angles (mean)	Calculated angles	Theoretical angles
$\theta_{oa}=20°02'$ $\theta_{ob}=21°36'$ $\theta_{oc}=21°14'$	$\delta_{OA}=20°02'$ $\delta_{OB}=21°36'$ $\delta_{OC}=21°14'$	$(0001)/(10\bar{1}4)=21°30'$
	$\delta_{AB}=35°37'$ $\delta_{BC}=36°30'$ $\delta_{CA}=36°08'$	$(10\bar{1}4)/(\bar{1}104)=37°00'$
$\omega_{ab}=118°40'$ $\omega_{bc}=118°08'$ $\omega_{ca}=123°12'$		$120°00'$
$\theta_{oa}=26°53'$ $\theta_{ob}=26°50'$ $\theta_{oc}=27°10'$	$\delta_{OA}=26°53'$ $\delta_{OB}=26°50'$ $\delta_{OC}=27°10'$	$(0001)/(10\bar{1}3)=27°40'$
	$\delta_{AB}=45°50'$ $\delta_{BC}=46°35'$ $\delta_{CA}=46°20'$	$(10\bar{1}3)/(\bar{1}103)=47°30'$
$\omega_{ab}=119°28'$ $\omega_{bc}=121°00'$ $\omega_{ca}=119°52'$		$120°00'$

Table 3. Measured angles between various points of $(11\bar{2}0)$ light figure of sapphire crystal.

Calculated angles
$\delta_{AB}=21°24'$ $\delta_{BC}=26°50'$ $\delta_{CD}=22°40'$ $\delta_{DA}=25°30'$ $\delta_{AC}=36°29'$ $\delta_{BD}=31°53'$

surfaces. Fig. 6 shows triangular [0001] etch pits with $[11\bar{2}0]$ sides, showing three-fold symmetry. Their base is [0001] plane, which and other low-indices faces form a truncated regular triangular cone. It is to be noted that, when a [0001] surface as millor-polished by using a high-velocity millor polisher with an alumina plate was etched, etch pits of regular triangular cone were revealed (Fig. 7). The [0001] light figure corresponding the former [0001] etch pits are more favourable for the crystal orientation determination than that corresponding to the latter [0001] etch pits. Next, $[11\bar{2}0]$ etch pits seem to have tetragonal symmetry, but it is found by a close examination that it is naturally not the case. These etch pits are lens-shaped, of which the axis is along the [0001] direction. Finally, Fig. 9 shows the

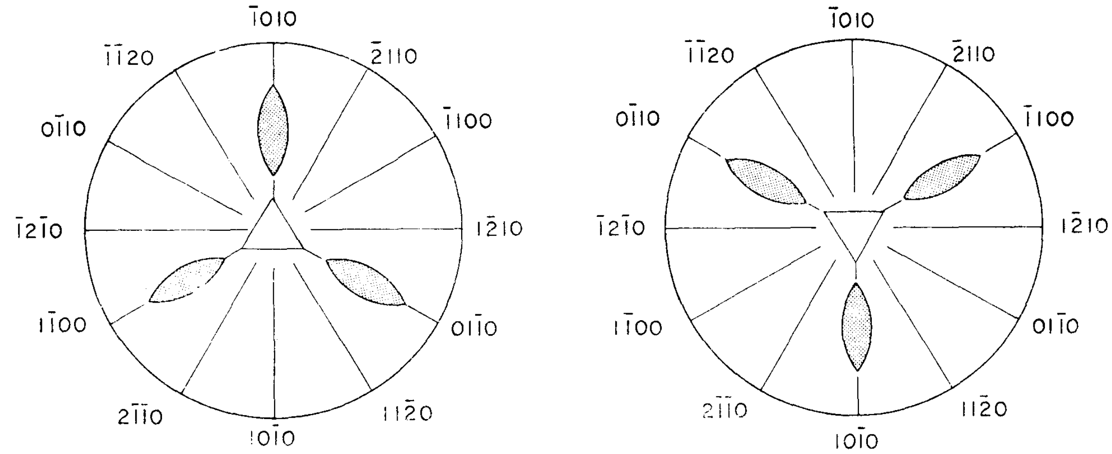

Fig. 12. Relationship between [0001] etch pits and light figures.

spatial relationship among the above-mentioned etch pits.

Light figures revealed by the etch [0001] and [11$\bar{2}$0] surfaces were observed by Yamamoto's crystal orientation determining apparatus(5). The results are shown in Figs. 10 and 11. Further, with [0001] and [11$\bar{2}$0] light figures, angular relations was measured using a two-circle goniometer in order to determine the symmetry of the light figure and of crystal facts constituting the corresponding etch pits, of which the results are shown in Tables 2 and 3. From these tables, it can be seen that [0001] etch pits have three-fold symmetry and that their base plane is [0001] plane, while their side planes are relatively low indices planes such as [10$\bar{1}$4], [10$\bar{1}$3], etc. Also it is seen that [11$\bar{2}$0] etch pits and corresponding light figure have two-fold symmetry.

Symmetry relations of the etch pits and of the corresponding light figures found from the above-mentioned observational results are such as shown in Fig. 12.

It is to be noted, finally, that the conditions necessary to reveal light figures and etch pits which are most appropriate for orientation determination are to be examined further. It is to be emphasized, however, that the crystal orientation of sapphire can be determined simply and accurately by the light-figure method(5).

Acknowledgements

We are very glad to say thanks to Professor Takao Iwata for the establishment of the Vernouil equipment used and to Professor Jirô Watanabé for the light-figure method.

(5) M. Yamamoto, J. Inst. Met. Japan, **5** (1941), 214 (in Japanese); Sci. Rep. Tohoku Imp. Univ., **31** (1943), 121.